



# The effect of excess air on combustion behaviors in vertical pulverized biomass burner

Aphichon Mungchu, Anuwat Saenpong, Kumpanat Chaiphet,  
Keyoon Duanguppama, Chinnapat Turakarn\*

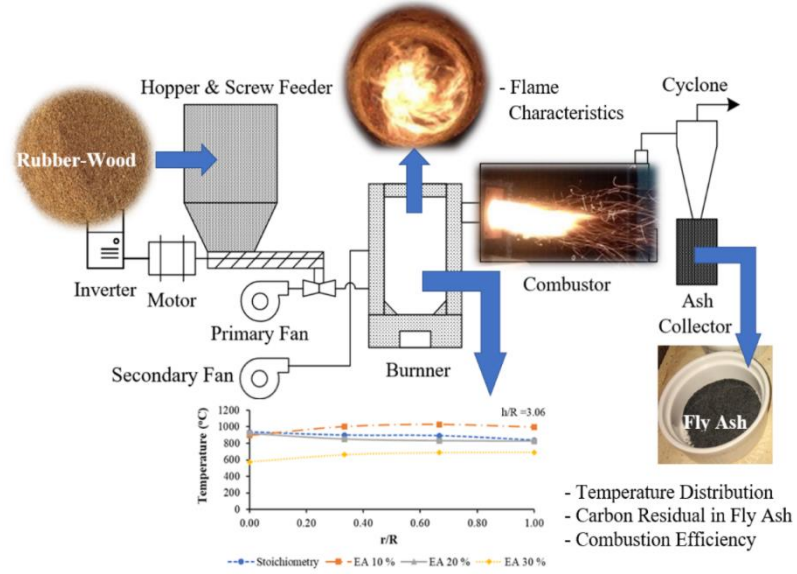
Department of Mechanical Engineering, Faculty of Engineering and Industrial Technology,  
Kalasin University, 46000 Thailand.

\*Corresponding Author: chinnapat.tu@ksu.ac.th  
<https://doi.org/10.55674/jmsae.v12i2.248089>

Received: 4 April 2022 | Revised: 21 April 2022 | Accepted: 13 February 2023 | Available online: 1 May 2023

## Abstract

The objectives of this research were to improve biomass burners to be suitable for horizontal fire tube boilers and to study the influence of stoichiometry, 10, 20 and 30% excess air with the air supply divided into two parts, including primary air and secondary air. Rubber wood sawdust was used as the biomass for this experiment. The biomass burners in this experiment had an internal diameter of 30 cm and a chamber height of 70 cm, which stand on the bottom ash bin, comprising combustion with a heating power of 150 kW and a 40:60 percent ratio of primary air to secondary air. The results showed that the burner was able to maintain a constant burning state when the temperature at which the fuel particles were fed into the burner was higher than the devolatilization temperature (400 °C). The introduction of secondary air into the center burner in a three-way rotation resulted in flame characteristics within the burner induced in the internal center arc of the burner by a radial ratio ( $r/R$ ) of 0.33 – 1. The radial ratio ( $r/R$ ) of 0.67 showed that the combustion reaction with 10% excess air had a maximum mean temperature distribution inside the burner of 1,000 °C. Combustion at 10% excess air had minimum residual carbon in the fly ash of 38.22% and a maximum combustion efficiency of 89.29%. As a result, such excess air was suitable as a condition used for vertical biomass burners.



**Keywords:** Burner; Pulverized biomass; Excess air

© 2023 Center of Excellence on Alternative Energy reserved

## Introduction

At present, a country's energy demand tends to increase as the country develops. Most of the energy sources come from fossil fuels such as coal, petroleum, and natural gas. These energy sources tend to run short and may run out, resulting in the crisis of continuously rising oil prices. In addition, the use of fossil fuels affects the environment and human daily living. Therefore, both the public and private sectors must search for renewable energy sources in various forms to replace fossil fuels to support their energy needs.

Several recognized potential energy sources include plastic waste energy [1 – 6] and biomass energy [7 – 12].

Thailand is an agricultural country, so there is a significant amount of agricultural waste or biomass produced, such as rubber wood, rice straw, corncobs, rice husks and sawdust, etc. This biomass can be processed into energy in a variety of ways, such as fuel gas [13 – 15], bio-oil [16 – 18], biochar [9, 11, 12] and direct combustion [19 – 22]. Direct combustion is an easy method to operate as

biomass can be burned as energy to feed into the system. For example, biomass can be used as fuel in a burner to heat a boiler system before using steam in various applications. Most boilers use oil as fuel. If biomass such as rubber wood sawdust could be applied instead of fuel oil, it would reduce dependence on fossil fuels. In addition, the use of biomass as fuel with proper burner technology results in complete combustion and low air pollution [19 – 22]. The combustion of fuel has three main components: fuel, oxygen in the air, and heat. For this reason, air and fuel input characteristics are important to combustion patterns.

Based on the aforementioned, this research focused on the design and construction of burners for biomass fuel from rubber-wood sawdust. An experimental study was conducted on the influence of excess air on combustion behavior in biomass burners. This behavior will lead to optimum combustion performance from the operation of the standing biomass burner. In the future, it is expected that these burners could be used for industrial and commercial applications.

## Materials and Methods

### Rubber wood sawdust feedstock

In this research, crushed rubber wood sawdust was selected as the fuel for the experiment, as shown in Fig. 1. Before starting the experiment, the fuel was exposed to the sun for three hours in the atmosphere. It was then sifted through a sieve with a 1.50 mm diameter hole. The properties of rubber wood sawdust are shown in Table 1, and the size of the rubber wood sawdust is shown in Table 2.



**Fig. 1** Rubber wood sawdust samples.

**Table 1** Properties of rubber–wood sawdust [23].

Proximate analysis (wt%)				As received base (MJ kg <sup>-1</sup> )		
Volatile		Fixed Carbon		Moisture		Ash
76.80		15.20		5.80		2.20
Ultimate analysis (wt%)						
C	H	N	S	O	HHV	LHV
49.40	6.10	0.40	0	43.90	17.50	16.20

**Table 2** Size of rubber–wood sawdust fuel.

Size of fuel (μm)	(wt%)
≥ 1000	24
500 ≤ S ≤ 1000	40
250 ≤ S ≤ 500	16
125 ≤ S ≤ 250	10
53 ≤ S ≤ 125	6

For burning, rubber wood sawdust was tested at a heating power of 150 kW. Before testing, the elemental composition and calorific value of biomass were taken to calculate the fuel content, stoichiometry air volume and excess air volume for the combustion process. They were calculated according to correlation equations (1), (4), and (7), respectively [24 – 25]. The results of the calculations were used as the experimental conditions, as in Table 3.

The amount of fuel for combustion can be estimated by eq. (1);

$$m_{fuel} = \frac{\text{Thermal Throughput}}{LHV} \quad (1)$$

Where  $m_{fuel}$  = mass of fuel for combustion, *Thermal Throughput* = burner heating power (kW), and *LHV* = heat value of fuel (MJ kg<sup>-1</sup>)

The amount of oxygen for combustion can be estimated by eq. (2);

$$m_{O_2,Air} \left[ \frac{kg O_2}{kg fuel(waf)} \right] = \left( X_C \frac{M_{O_2}}{M_C} + \frac{X_H}{4} \frac{M_{O_2}}{M_H} + X_S \frac{M_{O_2}}{M_S} - X_O \right) (1 - X_{H_2O}) \lambda \quad (2)$$

Where

$m_{O_2,Air}$  = mass of oxygen in air,

$M_i$  = molecular mass of element i by  $M_C = 12$ ,  $M_H = 1$ ,  $M_S = 32$ , and  $M_{O_2} = 32$ .

$X_i$  = mass fraction of element i in dry ash-free fuel (daf).

$X_{H_2O}$  = mass fraction of H<sub>2</sub>O in wet ash-free fuel (waf).

$\lambda$  = excess air ratio.

Nitrogen content can be estimated by eq. (3);

$$m_{N_2,Air} \left[ \frac{kg N_2}{kg fuel (waf)} \right] = m_{O_2,Air} \frac{Y_{N_2,Air}}{Y_{O_2,Air}} \frac{M_{N_2}}{M_{O_2}} \quad (3)$$

Where  $Y_{O_2,Air}$  = volume fraction of  $O_2$  in air (usually assumed to be 0.21),  $Y_{N_2,Air} = 1 - Y_{O_2,Air}$ , and  $Y_{N_2,Air} = 1 - Y_{O_2,Air}$

Air volume for combustion can be estimated by eq. (4);

$$m_{Air} \left[ \frac{kg air}{kg fuel (waf)} \right] = m_{O_2,Air} + m_{N_2,Air} \quad (4)$$

The stoichiometric air-fuel ratio can be estimated by eq. (5);

$$(A/F)_{stoic} = \left( \frac{m_{air}}{m_{fuel}} \right) \quad (5)$$

The equivalence ratio can be estimated by eq. (6);

$$\Phi = \frac{(A/F)_{stoic}}{(A/F)} \quad (6)$$

Percent excess air (EA) can be estimated by eq. (7);

$$\% excess air (EA) = \frac{(1 - \Phi)}{\Phi} \times 100\% \quad (7)$$

**Table 3.** Experimental conditions

Experimental conditions	Value
Thermal Throughput (kW)	150
Fuel feed rate ( $kg \ min^{-1}$ )	0.56
Primary air (%)	40
Secondary air (%)	60
Stoichiometry air volume flow rate ( $m^3 \ min^{-1}$ )	2.63
10% excess air volume flow rate ( $m^3 \ min^{-1}$ )	2.89
20% excess air volume flow rate ( $m^3 \ min^{-1}$ )	3.16
30% excess air volume flow rate ( $m^3 \ min^{-1}$ )	3.42

#### Equipment

Fig. 2 shows a schematic diagram of the biomass fuel combustion experiment kit in this research, which consists of three main components as follows:

1) The hopper and screw feeder can continuously control the fuel feed rate by adjusting the speed of the screw conveyor [26].

2) The vertically placed biomass burner has an internal diameter for the combustion chamber of 30 cm and a chamber height of 70 cm (90 cm measured from the ground)

which stands on the bottom ash bin. Considering Fig. 3, the air supplied inside the burner was divided into two parts. Primary air was the air that carried fuel from the screw conveyor to the bottom of the burner, while secondary air was fed to the center burner in a three-way swirling air system. This provided a high flow rate of hot gas with high turbulence. The mixture of fuel and air provided combustion efficiency at high heat rates [27].

3) The exhaust gas treatment system consists of the cyclone and the wet scrubber. The fly ash contained within the unburnt char of the cyclone was analyzed for residual carbon content.

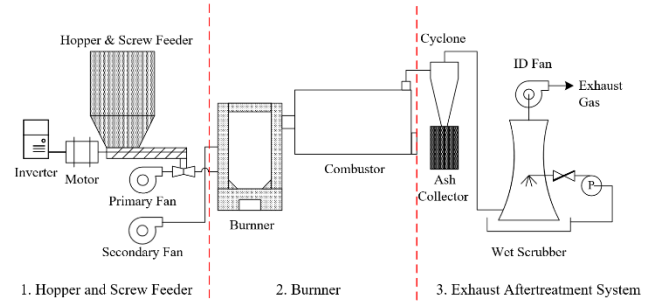


**Fig. 2** Diagram of biomass fuel combustion experiment unit.

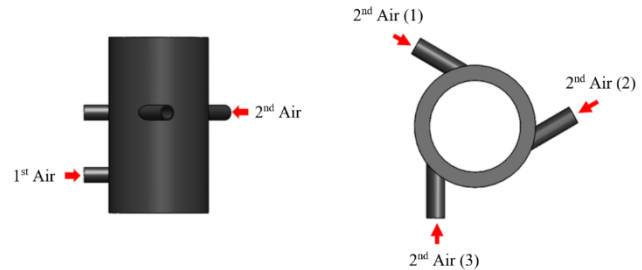


**Fig. 3** Positions for primary air and secondary air.

#### Method

The influence of excess air on combustion behavior was studied for diffusion temperature and the temperature inside the burner. Thermocouple type k was used to measure temperature and record all 20 points in the Graphtec midi LOGGER GL840 to study the complete combustion for the fuel burner, as shown in Fig. 4.

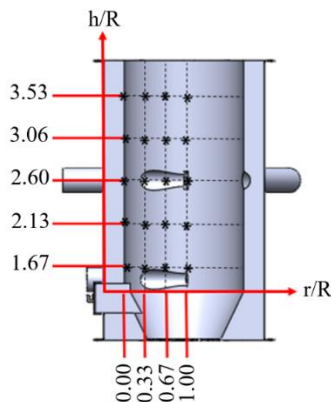


**Fig. 4** Position of temperature records inside biomass fuel burners.

1) Experimenting began using stoichiometry conditions. The biomass burner was then heated with an LPG pilot burner to ignite the flame. After that, the primary air compressor was initiated and the temperature rise was observed.

2) When the temperature of the burner wall reached 300 °C, the secondary air compressor was started by adjusting the ratio of the primary air to 40% and the secondary air to 60%. As for the air volume, 40% of the first section was the minimum amount of air that could continually carry fuel from the screw conveyor to the bottom of the burner.

3) The biomass fuel screw conveyor was operated and the rotation speed of the screw conveyor was adjusted to achieve a fuel feed rate of  $0.56 \text{ kg min}^{-1}$ .

4) When the temperature inside the burner was stable, the appearance of the flame occurring inside the burner and the burner outlet pipe was recorded. The temperature of the burner inside and the outlet temperature of one hot gas were recorded, as well as a sample of ash at the bottom of the cyclone to further analyze the remaining carbon content in fly ash and combustion efficiency.

## Results and Discussions

### Combustion behavior in biomass burners

Preheating of the fuel burner with liquefied petroleum gas was done by feeding air in the direction of the burner's tangential contact. As a result, the natural flames that occurred inside the burner were swirling and touching the surrounding wall inside the burner, as shown in Fig. 5. When the temperature of the wall inside the burner rose to 300 °C, the biomass fuel was fed to the burner along with a portion of the air, while secondary air was fed to the center burner

in a three-way swirling air system. As a result, the natural flames inside the burner were induced to spin in the internal center region of the biomass fuel burner, as shown in Fig. 6.

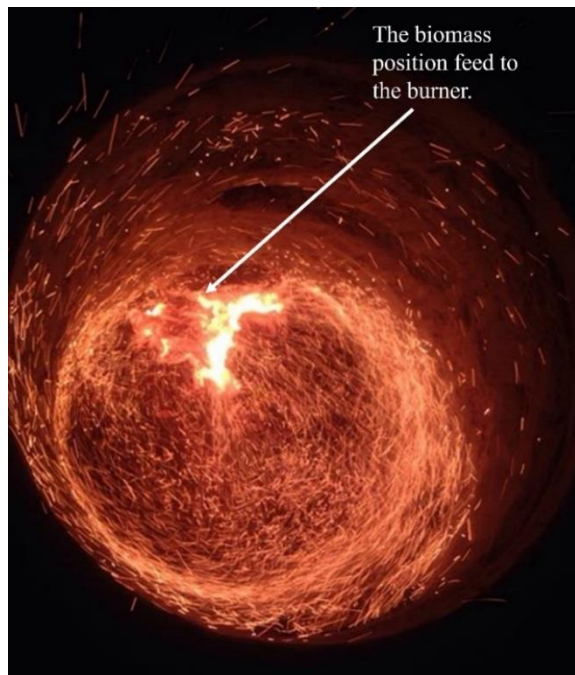


**Fig. 5.** The behavior of internal air circulation while warming the burner.



**Fig. 6** Rotating behavior of the flame in the center of the burner.

Fig. 7 shows that the temperature distribution inside the burner at the stoichiometry conditions and 10%, 20% and 30% excess air at the height ratio  $h/R = 1.67$ , the temperature in the area was higher than 800 °C. This shows that volatile

matter was released and the combustion reaction was instantaneous when the fuel was fed into the burner in the drying process. As a result, the burner can maintain a constant burning state. In addition, the volatile combustion reaction continued and became more intense at a height ratio of  $h/R = 2.13$ . This caused the temperature inside the burner to rise above  $900^\circ\text{C}$ . This temperature also causes the particles in the biomass to start a combustion reaction and the behavior of the primary air was spinning around the circumference of the burner. As a result, the radial temperature distribution at this height ratio was relatively uniform. The combustion conditions at 10% excess air had a maximum average temperature of  $920^\circ\text{C}$ , while 30% excess air for the combustion condition had the lowest mean temperature of  $815^\circ\text{C}$ .

The height ratio of  $h/R = 2.60$  was where the secondary air was fed into the three-way rotating burner. The char particles were thus induced into a combustion reaction in the center of the burner between the position of the radius ratio  $r/R = 0.33 - 1$ , which can be seen from the flame characteristics in Fig. 7. However, the second mass of air with low temperature causes the combustion reaction to slow down. The temperature at a height ratio of  $h/R = 2.60$  was lower, especially near the burner wall between the radius ratio  $r/R = 0 - 0.33$ . Stoichiometry air experiment conditions resulted in the least decrease in temperature near the combustion chamber wall. This is because the mass of air fed into the burner was small compared to other experimental conditions. In other words, the wall temperature drop was proportional to the amount of air entering the burner, while at a radial ratio of  $r/R = 0.33 - 1$ , 10% excess air still had a maximum average temperature distribution of  $984^\circ\text{C}$ .

When the second volume of air was added, it resulted in the re-combustion reaction at height ratios of  $h/R = 3.06$  and  $h/R = 3.53$ . The amount of oxygen in the air was sufficient to burn the charcoal. This results in a higher temperature distribution inside the burner, especially at a radial ratio between  $r/R = 0.33 - 1$ . The 10% excess air condition still gave a higher mean temperature distribution than other excess air conditions. The maximum combustion temperature was achieved at  $1,035^\circ\text{C}$  at a height ratio of  $h/R = 3.53$  and a radial distance ratio of  $r/R = 0.67$ . The temperature distribution inside the burner was compared and rated at  $h/R = 3.53$ . It was found that the 10% excess air combustion condition had the highest mean temperature distribution of  $1,000^\circ\text{C}$ , followed by the stoichiometry air combustion condition and burning at 20% excess air,

respectively. In the combustion conditions at 30% excess air, the average minimum temperature distribution was  $632^\circ\text{C}$ .

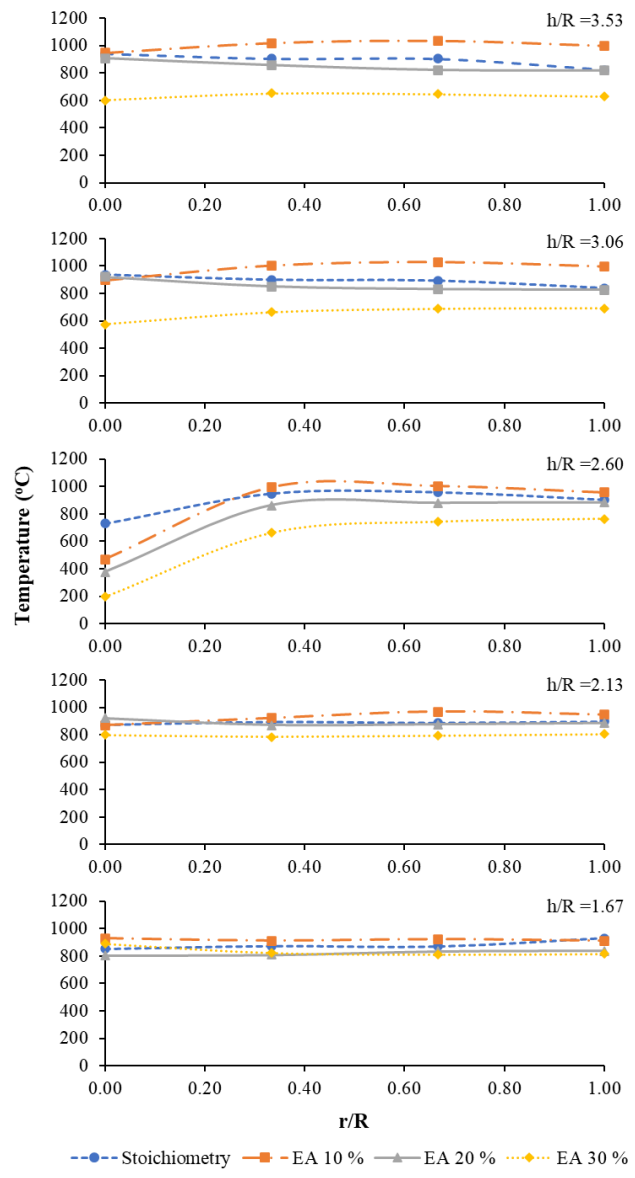


**Fig. 7** The temperature distribution inside the burner at theoretical climate conditions of 10%, 20% and 30% excess air, and a ratio of primary air to secondary air at 40:60.

When the temperatures at different locations for all height ratios of  $h/R = 1.67, 2.13, 2.60, 3.06$  and  $3.53$  were compared, the highest temperatures for hot gas combustion in each altitude ratio were  $929, 969, 1,003, 1,025$ , and  $1,035^\circ\text{C}$ , respectively. In all five cases, the high temperature was generated at a radial ratio of  $r/R = 0.67$ , indicating that the intensity of combustion was caused by both circumferential centrifugation and the three-way rotation of the air. Fig. 8 shows that 10% excess air had the highest flue

gas temperature at 925°C, followed by stoichiometry air and 20% excess air, respectively. For combustion conditions with 30% excess air, the lowest flue gas temperature was 555°C. This corresponds to the distribution of the combustion temperature inside the burner at  $h/R = 3.53$ .

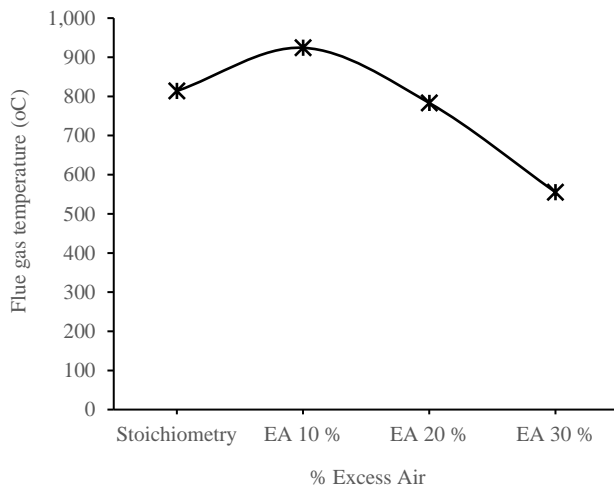


**Fig. 8** The influence of excess air on the temperature of the flue gas at the outlet of the burner.

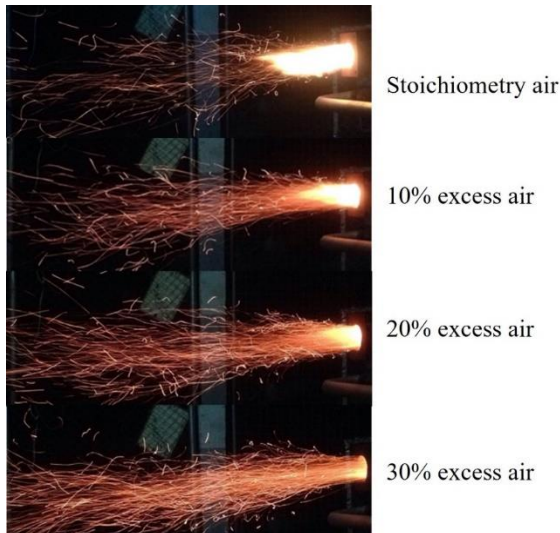


**Fig. 9** Influence of excess air on flame characteristics ejected from the burners.

#### Burner flame characteristics

The flame ejected from the burner in Fig. 9 was caused by the burning of rubber wood sawdust fuel inside the burner. It was found that the burning of the smaller fuel inside the burner, while the larger fuel would come out simultaneously with flue gas ejected by the wind being fed into the burner. This indicated that the residence time in the

combustion reaction of large fuel particles within the burner was insufficient. This is consistent with research by Akio Nishiyama [28], which indicated that the combustion of dust biomass fuels was suitable for fuel particles up to 500  $\mu\text{m}$  in size.

Comparing the burning conditions in which excess air was compared to the characteristics of the flame ejected from the burner, it was found that the length of the flame ejected was inversely proportional to the amount of excess air. That is, as the excess air increases, the length of ejected flame decreases. This is because the secondary air which is fed into the center burner in a three-way rotation induces combustion at the internal center of the burner. Excess air is more capable of inducing a reaction inside the burner, which is why the length of the flame is reduced. This is consistent with Abdallah's [29] research findings that showed increasing excess air leads to reduced jet development, increasing the flame temperatures, and reducing the lengths of visible flames.

Conversely, the intensity of particle centrifugation increased as excess air was added, resulting in a combustion reaction outside the burner due to the release of large fuel particles. This can be seen by the large amounts of sparks from the fuel particles ejected in the flames. In a flame of this nature, it is possible for incompletely burnt char particles to flow with the fly ash.

#### Analysis of carbon residual in fly ash and combustion efficiency

Carbon residual analysis is the application of the ash determination method in fly ash samples collected from the lower part of the cyclone. The experiment was conducted following ASTM D 3174 by weighing the fly ash sample, which was then sintered at 750°C for 4 h until the carbon was completely burned. After that, the ash was weighed again and the difference in weight loss was the amount of carbon remaining.

The experiment could not measure the amount of carbon monoxide from the composition of the exhaust gas. Therefore, the combustion efficiency could be calculated only by eq. (8) considering the heat lost to the non-burned fuel particles per the calorific value of the fuel fed to the burner. In the combustion of fuel, more than 90% of the unburned carbon was in the form of unburned char with heavy ash and fly ash [30].

$$\text{Combustion Efficiency } (\eta_{\text{comb}}) = 100 - \frac{\text{flue heat losses}}{\text{fuel heating value}} \times 100 \quad (8)$$

The heat lost to unburned fuel particles can be calculated by eq. (9);

$$\text{flue heat losses} = \dot{m}_{\text{unburn}} \times H_{\text{burnout}} \quad (9)$$

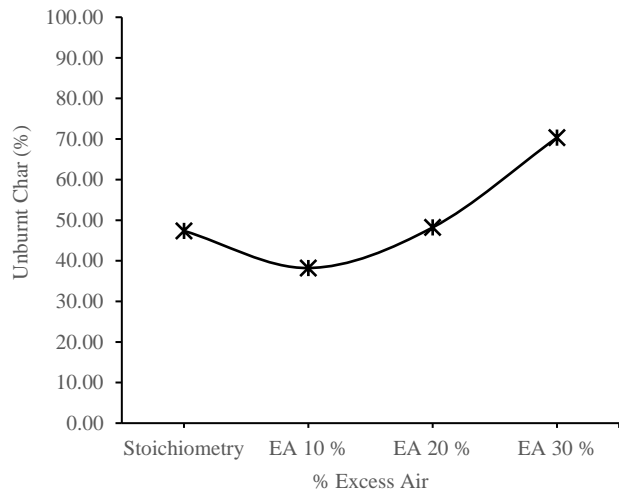


**Fig. 10** Influence of excess air on carbon residual in the fly ash.

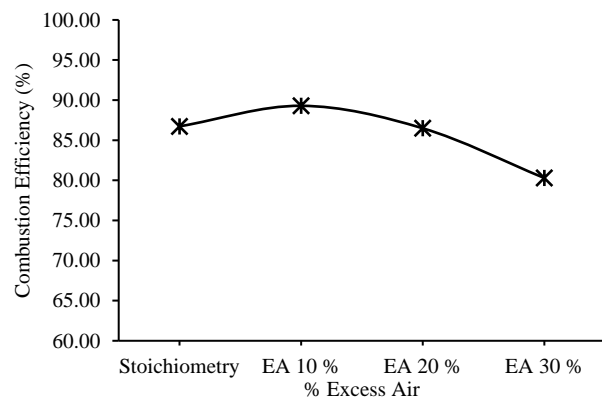


**Fig. 11** The influence of excess air on combustion efficiency.

Fig. 10 shows that 10% excess air has the least carbon residual in the fly ash at 38%, while the theoretical air has 47% residual carbon, and 20% excess air has residual carbon at 48%. In 30% excess air, the highest amount of residual carbon in the fly ash was found at 70%. When the remaining carbon content in fly ash was calculated to estimate the combustion efficiency in Fig. 11, it was found that 10% excess air had the highest combustion efficiency of 89.29%. The Fig.s for the distribution of residual carbon in fly ash and combustion efficiency indicated that 10% excess air was

the most suitable for the combustion characteristics in the stand-up biomass burners.

## Conclusion

When the temperature at which the fuel particles are fed into the burner was higher than the devolatilization temperature (400 °C), the burner was able to maintain a constant burning state. The introduction of secondary air into the center burner in a three-way rotation resulted in flame characteristics within the burner induced in the internal center arc of the burner by a radial ratio ( $r/R$ ) of 0.33 – 1. However, the temperature near the wall of the combustion chamber decreased, which was proportional to the volume of the secondary air being fed into the burner. The radial ratio ( $r/R$ ) of 0.67 showed that the combustion reaction was intense in the area, with 10% excess air having a maximum mean temperature distribution inside the burner of 1,000 °C, while the height ratio ( $h/R$ ) of 3.53 had the highest flue gas temperature at the burner exit of 925°C. The length of the flame emanating from the burner was inversely proportional to the amount of excess air. Increased excess air resulted in the length of the ejected flame being reduced. In addition, a large excess of air resulted in more micro-particles from burning biomass coming off as flakes. In this kind of flame, smaller char particles may have a chance to escape with the fly ash. Combustion at 10% excess air conditions had a minimum residual carbon in fly ash of 38.22% and a maximum combustion efficiency of 89.29%. As a result, such excess air was suitable for use as a condition for stand-up biomass burners. The proper proportion of air was primary air at 40% and secondary air at 60%.

## Acknowledgement

Thank you to the Department of Mechanical Engineering, Faculty of Engineering and Industrial Technology, Kalasin University, that provides assistance to equipment, tools and places to conduct research.

## References

- [1] K. Duanguppama, K. Chaiphet, P. Kraisoda, C. Turakarn, Fuel production from plastic waste with fast pyrolysis, The First National and International Conference of Kalasin University 2019, Kalasin University. 15 – 16 July 2019, 82 – 90.
- [2] K. Chaiphet, C. Turakarn, S. Pongskul, K. Duanguppama, Effect of plastic type on the yields and properties of fuel from fast pyrolysis, The 11th

Engineering, Science, Technology and Architecture Conference 2020, Nakhon Ratchasima Rajabhat University. 21 August 2020, 1296 – 1302.

[3] C. Turakarn, K. Chaiphet, K. Suwanapa, K. Duanguppama, The effect of pyrolysis temperature on yields and properties of fuel from plastic bag, The 11th Engineering, Science, Technology and Architecture Conference 2020, Nakhon Ratchasima Rajabhat University. 21 August 2020, 566 – 571.

[4] C. Turakarn, K. Duanguppama, K. Chaiphet, A. Mungchu, S. Boothaisong, S. Phokha, The Effect of Plastic Waste Oil from Fast Pyrolysis Process on Lowest Brake Horsepower and Maximum Engine Brake Specific Fuel Consumption, *J – REC.* 4(2) (2021) 14 – 20.

[5] K. Chaiphet, C. Turakarn, K. Duanguppama, C. Sasen, S. Khamsuwan, P. Promphiphha, The product yields and fuel properties from catalytic pyrolysis of plastic bag, *J. Mater. Sci. Appl. Energy.* 11(1) (2022) 16 – 23.

[6] M. Kusenberg, A. Eschenbacher, M.R. Djokic, A. Zayoud, K. Ragaert, S. De Meester, K.M. Van Geem, Opportunities and challenges for the application of post-consumer plastic waste pyrolysis oils as steam cracker feedstocks: To decontaminate or not to decontaminate?, *Waste Manag.* 138 (2022) 83 – 115.

[7] B. Freel, R. Graham, Method and apparatus for a circulating bed transport fast pyrolysis reactor system, U.S. Patent No. 5,792,340, Washington, DC., 1998.

[8] A.V. Bridgwater, Upgrading biomass fast pyrolysis liquids, *Environ. Prog. Sustainable Energy.* 31(2) (2012) 261 – 268.

[9] D. Chen, A. Gao, K. Cen, J. Zhang, X. Cao, Z. Ma, Investigation of biomass torrefaction based on three major components: Hemicellulose, cellulose, and lignin, *Energ Convers Manag.* 169 (2018) 228 – 237.

[10] T.J. Morgan, A. Youkhana, S.Q. Turn, R. Ogoshi, M. Garcia-Pérez, Review of Biomass Resources and Conversion Technologies for Alternative Jet Fuel Production in Hawai'i and Tropical Regions, *Energ Fuel.* 33(4) (2019) 2699 – 2762.

[11] Y. Niu, Y. Lv, Y. Lei, S. Liu, Y. Liang, D. Wang, S.E. Hui, Biomass torrefaction: properties, applications, challenges, and economy, *Renew Sustain Energ Rev.* 115 (2019) 109395.

[12] M.N. Cahyanti, T.R.K.C. Doddapaneni, T. Kikas, Biomass torrefaction: An overview on process parameters, economic and environmental aspects and recent advancements, *Bioresource Technol.* 301 (2020) 122737.

[13] O. Yakaboylu, J. Harinck, K.G. Smit, W. de Jong, Testing the constrained equilibrium method for the modeling of supercritical water gasification of biomass, *Fuel Process Tech.* 138 (2015) 74 – 85.

[14] D. Barisano, G. Canneto, F. Nanna, E. Alvino, G. Pinto, A. Villone, M. Carnevale, V. Valerio, A. Battafarano, G. Braccio, Steam/oxygen biomass gasification at pilot scale in an internally circulating bubbling fluidized bed reactor, *Fuel Process Tech.* 141 (2016) 74 – 81.

[15] J. Billaud, S. Valin, M. Peyrot, S. Salvador, Influence of H<sub>2</sub>O, CO<sub>2</sub> and O<sub>2</sub> addition on biomass gasification in entrained flow reactor conditions: Experiments and modelling, *Fuel.* 166 (2016) 166 – 178.

[16] K. Duanguppama, A. Pattiya, Fast pyrolysis of Leucaena leucocephala in a circulating fluidised bed reactor, 23rd European Biomass Conference and Exhibition 2015, Vienna, Austria. 1 – 4 June 2015, 1206 – 1211.

[17] K. Duanguppama, N. Suwapaet, A. Pattiya, Fast pyrolysis of contaminated sawdust in a circulating fluidised bed reactor, *J Anal Appl Pyrol.* 118 (2016) 63 – 74.

[18] K. Duanguppama, K. Rueangsan, P. Kraisoda, C. Turakarn, The effect of catalyst on the heating value and energy yield from the fast pyrolysis of leucaena leucocephala, *UDRU Sci. & Tech. J.* 5(1) (2017) 97 – 111.

[19] A. Garcia-Maraver, J.A. Perez-Jimenez, F. Serrano-Bernardo, M. Zamorano, Determination and comparison of combustion kinetics parameters of agricultural biomass from olive trees, *Renew Energ.* 83 (2015) 897 – 904.

[20] J. Riaza, J. Gibbins, H. Chalmers, Ignition and combustion of single particles of coal and biomass, *Fuel.* 202 (2017) 650 – 655.

[21] M.A. Saeed, G.E. Andrews, H.N. Phylaktou, B.M. Gibbs, Flame speed and K<sub>st</sub> reactivity data for pulverised corn cobs and peanut shells, *J Loss Prev Process Indust.* 49 (2017) 880 – 887.

- [22] N. Sousa, J.L. Azevedo, Model simplifications on biomass particle combustion, *Fuel*. 184 (2016) 948 – 956.
- [23] P. Laphirattanakul, J. Charoensuk, C. Turakarn, C. Kaewchompoo, N. Suksam, Development of pulverized biomass combustor with a pre-combustion chamber, *Energy*. 208 (2020) 118333.
- [24] J. Koppejan, S. Van Loo, *The handbook of biomass combustion and co-firing*, 1st ed., Routledge, London, 2007.
- [25] R.T. Stephen, *An introduction to combustion: concepts and applications*, third ed., McGraw-Hill Companies, Incorporated, 2012.
- [26] M. Kamal, Parametric study of combined premixed and non-premixed flame coal burner, *Fuel*. 87(8-9) (2008) 1515 – 1528.
- [27] S. Jugjai, N. Polmart, Enhancement of evaporation and combustion of liquid fuels through porous media, *Exp Therm Fluid Sci.* 27(8) (2003) 901 – 909.
- [28] A. Nishiyama, H. Shimojima, A. Ishikawa, Y. Itaya, S. Kambara, H. Moritomi, S. Mori, Fuel and emissions properties of Stirling engine operated with wood powder, *Fuel*. 86(15) (2007) 2333 – 2342.
- [29] A. Elorf, B. Sarh, Excess air ratio effects on flow and combustion characteristics of pulverized biomass (olive cake), *Case Studies in Thermal Engineering*. 13 (2019) 100367.
- [30] C. Turakarn, *Biomass Burner Development in Industrial Boilers*, M.Eng. Mechanical Engineering, King Mongkut's Institute of Technology Ladkrabang, Bangkok, 2015.